Current Applied Physics 18 (2018) 1225–1229

Contents lists available at ScienceDirect

Current Applied Physics

journal homepage: www.elsevier.com/locate/cap

Resonant inelastic X-ray scattering of tantalum double perovskite structures

Ju Hyun Oh[a], Jung Ho Kim[b], Jung Hyun Jeong[a], Seo Hyoung Chang[a,c,*]

[a] Department of Physics, Pukyong National University, Busan 48513, South Korea
[b] Advanced Photon Source, Argonne National Laboratory, Lemont 60439, United States
[c] Department of Physics, Chung-Ang University, Seoul 06974, South Korea

ARTICLE INFO

Keywords:
Resonant inelastic X-ray scattering
$SrLaMgTaO_6$
Double perovskites
Light emitting diodes

ABSTRACT

In this paper, we investigated the electronic structures and defect states of $SrLaMgTaO_6$ (SLMTO) double perovskite structures by using resonant inelastic x-ray scattering. Recently, Eu^{3+} doped SLMTO red phosphors have been vigorously investigated due to their higher red emission efficiency compared to commercial white light emitting diodes (W-LED). However, a comprehensive understanding on the electronic structures and defect states of host SLMTO compounds, which are specifically related to the W-LED and photoluminescence (PL), is far from complete. Here, we found that the PL spectra of SLMTO powder compounds sintered at a higher temperature, 1400 °C, were weaker in the blue emission regions (at around 400 nm) and became enhanced in near infrared (NIR) regions compared to those sintered at 1200 °C. To elucidate the difference of the PL spectra, we performed resonant inelastic x-ray spectroscopy (RIXS) at Ta L-edge. Our RIXS result implies that the microscopic origin of different PL spectra is not relevant to the Ta-related defects and oxygen vacancies.

1. Introduction

Although white light emitting diodes (W-LEDs) were successfully fabricated by using a yellow phosphor (YAG:Ce) coated on the blue LED chips, the white light with a combination of blue and yellow has a drawback: it exhibits high correlated color temperature (CCT) and low color rendering indices (CRI) due to deficiency of the red light (above 600 nm) [1–5]. To overcome the drawback, many researchers have vigorously investigated and developed red phosphors with high efficiency and chemical stability. Of the many red phosphors, Eu^{3+} doped $SrLaMgTaO_6$ red phosphors have been reported to emit a higher red emission efficiency than the commercial Y_2O_3:Eu^{3+} red phosphors [6,7]. Nevertheless, the relationship between the photoluminescence (PL) spectra and relevant defect states of $SrLaMgTaO_6$ (SLMTO) host lattice (structure of formula AA'BB'O_6 [8,9]) needs further investigation in order to achieve the realization of W-LEDs with better CRI.

The physical and chemical properties of perovskite compounds are closely related to the oxygen vacancies, cation stoichiometry, the configuration of the A and/or B cations, and octahedral rotations [10,11]. For instance, small oxygen vacancies or cation stoichiometry can induce different electronic structures and defect states of the SLMTO compounds. Previous studies, however, lack direct experimental evidence and a clear understanding on how specific defect states in the SLMTO host lattice improves the red emission light in the photoluminescence (PL) spectra. Therefore, monitoring oxygen vacancies or element-specific defects in the compounds can unveil the microscopic origin of PL spectra.

Resonant inelastic x-ray scattering (RIXS) is a powerful tool to monitor the change of defect states related to the elements in SLMTO compounds [12]. As a photon-in and photon-out, RIXS at the Ta L_3-absoprtion edge (9.881 keV) is able to detect and verify electronic excitation in Tantalum double perovskite compounds in a non-destructive way. Ta ion in stoichiometric SLMTO has 5 + valency and 5d orbitals are fully unoccupied ($5d^0$). When oxygen vacancies near Ta ions exist, 5d orbitals were changed from unoccupied to partially occupied states. We thereby propose that RIXS at Ta L_3-absroption edge can detect and verify Ta 5d-related defect states inside the band gap of SLMTO.

In this article, we investigated the structural, electronic excitation, and photoluminescence (PL) properties of $SrLaMgTaO_6$ (SLMTO) powder compounds, which were sintered at 1200 °C and 1400 °C, respectively. X-ray diffraction measurements with Rietveld refinement analyses indicated that the two samples had the same monoclinic structure but showed small changes of the lattice parameters: less than 0.2%. SLMTO samples sintered at the higher temperature exhibited the stronger red-to-NIR emission band. Our resonant inelastic x-ray scattering (RIXS) studies clearly demonstrate that there are significant changes in the RIXS spectra, indicating little Ta-related oxygen vacancies in the SLMTO compounds. The findings of this study can contribute to the development of higher-efficiency double-perovskite phosphors, as the RIXS studies reveal the hidden relation between PL

* Corresponding author. Department of Physics, Pukyong National University, Busan 48513, South Korea.
E-mail addresses: cshyoung@pknu.ac.kr, cshyoung@cau.ac.kr (S.H. Chang).

https://doi.org/10.1016/j.cap.2018.05.014
Received 15 April 2018; Accepted 11 May 2018
Available online 15 May 2018

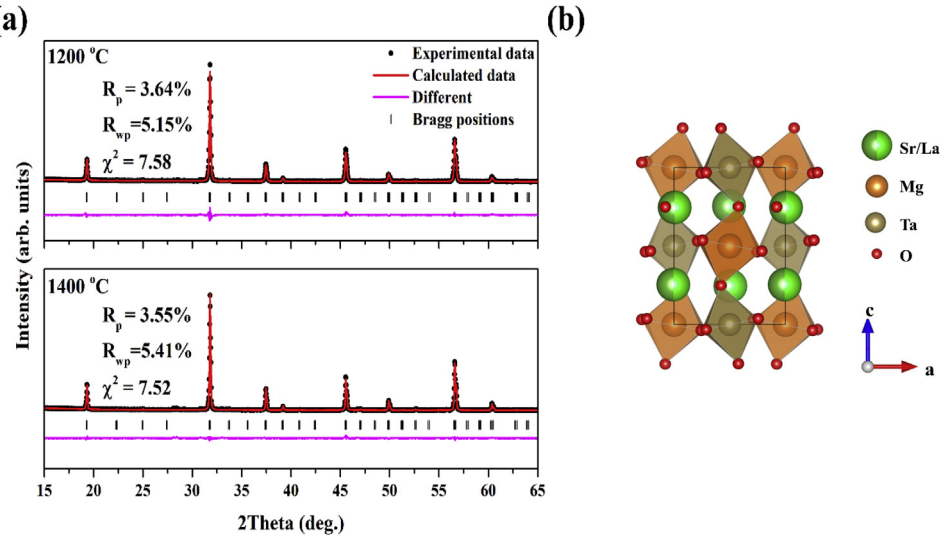

Fig. 1. X-ray diffraction (XRD) θ-2θ scan measurements and Rietveld of $SrLaMgTaO_6$ (SLMTO) powder samples sintered at different temperatures. (a) Temperature-dependence of SLMTO growth: 1200 °C (up) and 1400 °C (bottom). (b) Schematic of crystal structure of SLMTO double perovskite structure.

Table 1
Lattice parameters obtained from Rietveld refinement of XRD pattern for $SrLaMgTaO_6$ powders.

	$SrLaMgTaO_6$	
	1200 °C	1400 °C
a (Å)	5.639	5.635
b (Å)	5.629	5.639
c (Å)	7.958	7.965
α (°)	90	90
β (°)	89.98	90.01
γ (°)	90	90
V (Å^3)	252.6	253.1

characteristics and Ta-related defects of the double-perovskite host lattices.

2. Experimental methods

Polycrystalline ceramic samples with composition of $SrLaMgTaO_6$ (SLMTO) were synthesized by a conventional mix of oxide method employing the solid-state reaction of $SrCO_3$ (99.994%), La_2O_3 (99.99%), $(MgCO_3)_4Mg(OH)_2{\cdot}5H_2O$ (99.99%), and Ta_2O_5 (99.99%). All the reagents were purchased from Alfa-Aesar. The mixture of starting materials was mixed and ground in an agate mortar, then was calcined at 900 °C for 2 h. After that, the mixture was ground again, and sintered at 1200 °C and 1400 °C for 12hr, respectively. The SLMTO powder samples were supplied by the Functional Phosphor Bank at Pukyong National University (2017M3A9B8069470).

The crystal structures were analyzed using experimental X-ray diffraction (XRD) data and Rietveld refinement software (general structure analysis system, GSAS). XRD data were collected in the range of 10–80° for a scan speed of 2°/min using the X'Pert-MPD system (Panalytical, Netherland) with Cu $K\alpha_1$ radiation at a wavelength of 1.5406 Å. Energy-dispersive spectroscopy (EDS, HORIBA) attached to a scanning electron microscope (SEM, S-2700, HITACHI) was used for chemical composition analysis. The photoluminescence (PL) spectra were measured at room temperature and recorded with a fluorescence spectrophotometer (Acton SpectraPro 750-Triplet Grating Monochromator) from a charge-coupled device (CCD) detector (Princeton EEV 10241024 and PI-Max 133 controller). Resonant inelastic x-ray scattering (RIXS) and x-ray absorption spectroscopy (XAS) experiments were performed at the 27 ID beamline of Advanced Photon Source, Argonne National Laboratory. The details for RIXS measurements are presented elsewhere [13]. The use of the Advanced Photon Source at the Argonne National Laboratory was supported by the US DOE under Contract No. DE-AC02-06CH11357.

3. Results and discussions

The crystal structures of polycrystalline SLMTO powder samples were characterized by XRD θ-2θ scan measurements. As shown in Fig. 1(a), we synthesized and measured the XRD patterns of SLMTO samples sintered at different temperatures, 1200 °C and 1400 °C, respectively. We performed Rietveld refinement analyses based on the monoclinic structure with space group P21/n in the inorganic crystal

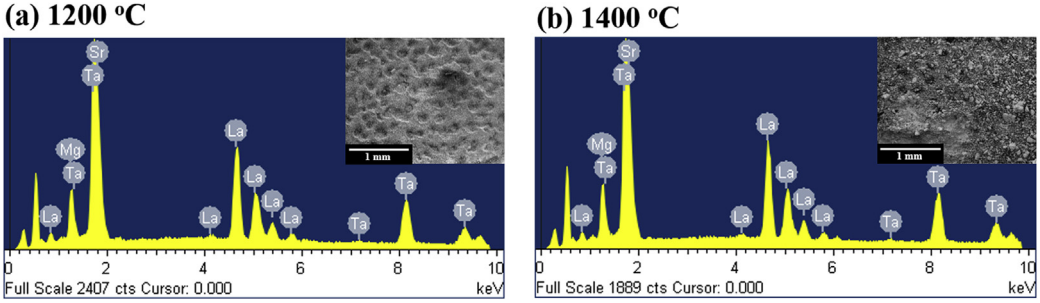

Fig. 2. Chemical and morphological properties of SLMTO. (a) Energy-dispersive x-ray spectra (EDS) of SLMTO powder sintered at 1200 °C. (b) EDS of the sample sintered at 1400 °C. The insets show scanning electron microscopic image with 1 mm scale bar.

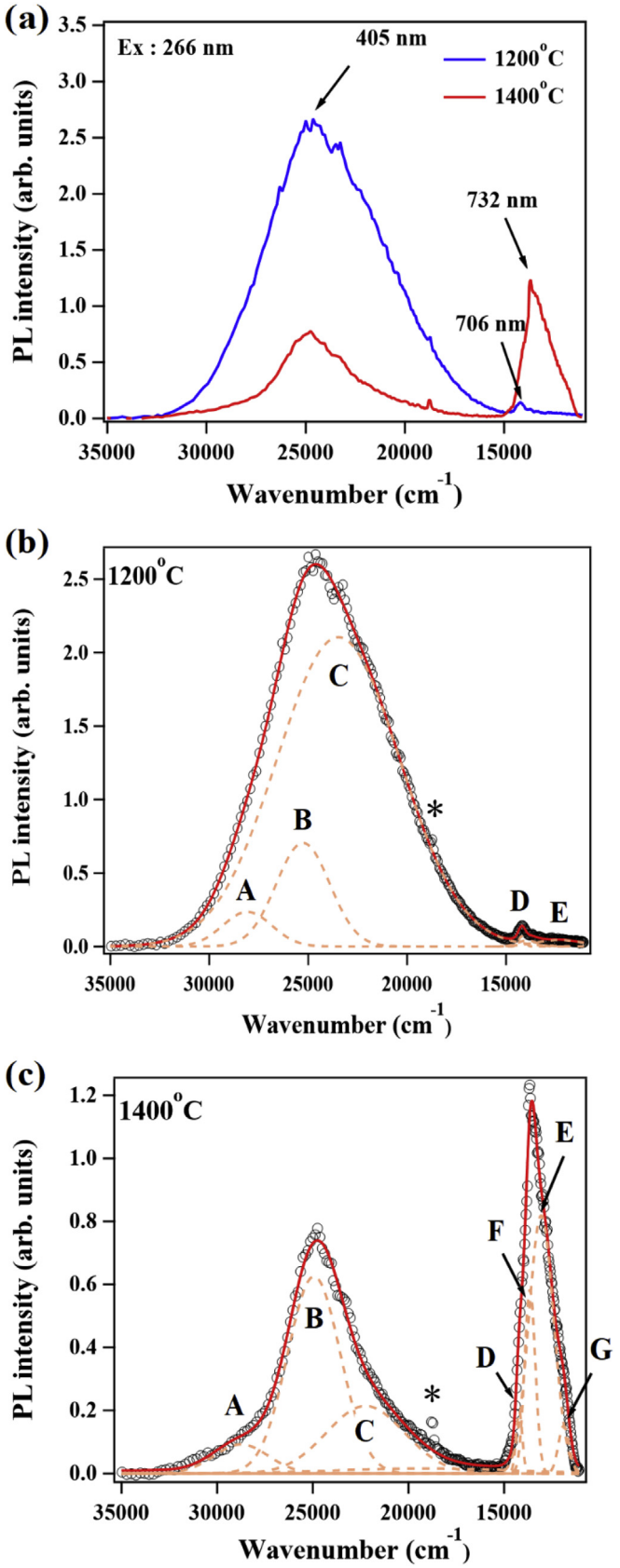

Fig. 3. Photoluminescence (PL) spectra of SLMTO powder. (a) The PL spectra of both samples sintered at 1200 °C (blue) and 1400 °C (red). (b) PL spectra with fitted and decomposed peaks of SLMTO samples sintered at (b) 1200 °C and (c) 1400 °C. Open black circles represent measured spectra, with fitted spectra and decomposed peaks represented by red solid line and dashed line, respectively. (For interpretation of the references to color in this figure legend, the reader is referred to the Web version of this article.)

structure database (ICSD). As shown in Table 1, the R factors (3–6%) of both samples show similar values, which are related to the quality and reliability of the fitting results [14–16]. The lattice parameters and volume of the sample sintered at different temperatures were very slightly changed to less than 0.2%; when increasing the sintering temperature, the lattice constant of *a* decreased while the *b* and *c* values increased.

As shown in Fig. 1(b), the Sr^{2+} and La^{3+} ions can be randomly distributed on the A site, and they are usually surrounded by twelve oxygen ions. Yet there are eight oxygen ions around the A site in this monoclinic system and four oxygen ions away from the A site (approximately above 0.3 nm) [17]. The Mg^{2+} and Ta^{5+} are orderly located on the B site surrounded by the oxygen octahedra. Most double-perovskite compounds have octahedral tilting distortion due to the mismatch between the ionic radius. The tolerance factor (t) represents the degree of the octahedral tilting distortion. The t value of SLMTO is calculated by the following relation,

$$t = (r_{sr} + r_o)/\sqrt{2}\,(r_{Mg,Ta} + r_o), \quad (1)$$

where $r_{Mg,Ta}$ is the average ionic radius of Mg^{2+} and Ta^{5+} ions. The t value of SLMTO compounds is 0.952 and thus octahedral tilting ($a^-a^-c^+$ tilting pattern) [8]. Owing to the small change of lattice parameters in the two samples, the octahedral tilting patterns can be maintained.

To check the possibilities of stoichiometry and morphology issues in the samples, we performed the energy-dispersive x-ray spectroscopy (EDS) as shown in Fig. 2. The EDS results displayed the presence of strontium (Sr), lanthanum (La), magnesium (Mg) and tantalum (Ta). Specifically, there were no other contaminated elements in both SLMTO powder samples. The inset of Fig. 2(a) and (b) displays the SEM images of SLMTO powders sintered at 1200 °C and 1400 °C, respectively. The crystal morphology and the particle size in both SLMTO powders can vary with different sintering temperature; the SLMTO powder sample sintered at 1400 °C exhibits a larger particle size than those of the sample sintered at 1200 °C.

To investigate the sintering temperature effects on the LED, we performed the PL spectra of SLMTO powder samples using a Nd:YAG laser as excitation source, as shown in Fig. 3(a). Under the excitation of 266 nm, the SLMTO powder samples showed drastically different PL spectra. For instance, the SLMTO powders sintered at 1200 °C have a strong and broad emission band centered at 405 nm and weak emission band centered at approximately 700 nm, comparted to that of the sample sintered at 1400 °C. In other words, the strong emission centered at 405 nm is weakened as the sintering temperature increases, whereas the emission band in NIR region (close to the red light) is enhanced.

To draw further insight on the physical origin of the emissions in the two regimes, we fitted the PL spectra of SLMTO powder samples, as shown in Fig. 3(b) and (c). Note that the peak at 532 nm (~18796 cm^{-1}) marked with an asterisk was excluded from Gaussian curve fitting because it is the second harmonic peak of Nd:YAG laser. Firstly, the broad emission band centered at 405 nm in the blue emission region is systematically decomposed into three components (peak A, B, and C) in both samples. These components are closely related to the emission bands of MgO [19]. Interestingly, the intensities of peak A and B are nearly similar in both samples, but the C component centered at 425 nm (~23480 cm^{-1}) show a quite different PL intensity depending on the samples. The intensity of peak C of the SLMTO sample

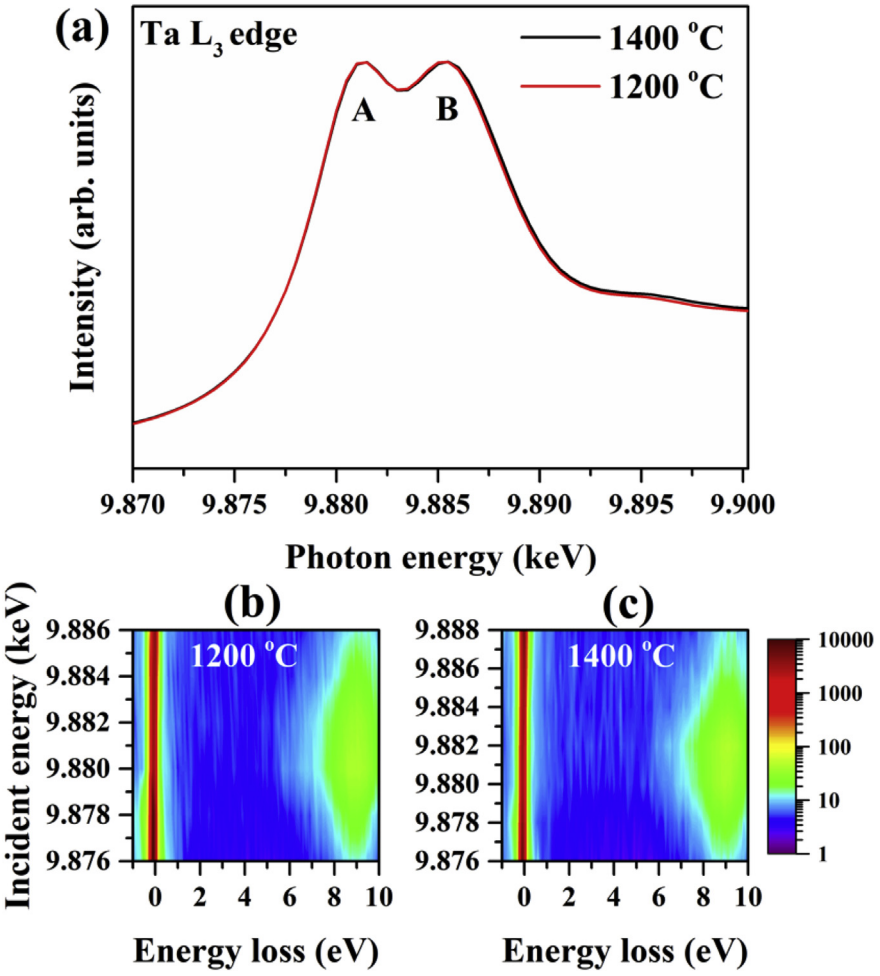

Fig. 4. X-ray absorption spectroscopy (XAS) and resonant inelastic x-ray scattering (RIXS). (a) Ta L_3-edge XAS spectra of SLMTO powder samples: 1200 °C (red) and 1400 °C (black). (b) RIXS spectra of SLMTO samples sintered at (b) 1200 °C and (c) 1400 °C as a function of the incident photon energy and energy loss. (For interpretation of the references to color in this figure legend, the reader is referred to the Web version of this article.)

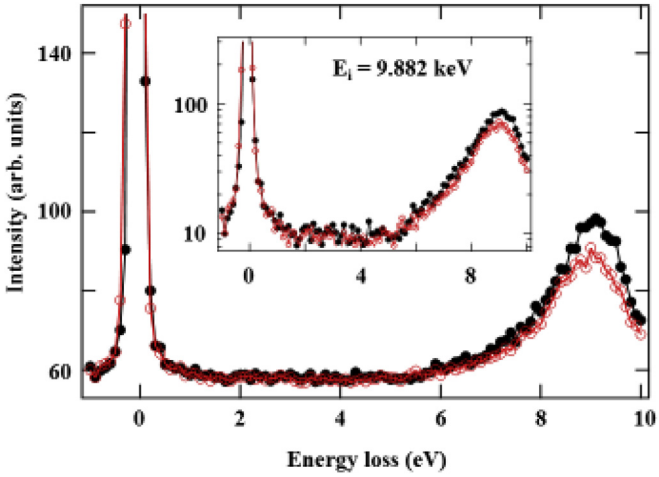

Fig. 5. Ta L_3-edge RIXS spectra. The RIXS spectra of SLMTO sintered at 1200 °C (red line) and 1400 °C (black line). The inset represents the same RIXS spectra with the logarithmic y-scale to clearly assign the band gap of SLMTO samples. (For interpretation of the references to color in this figure legend, the reader is referred to the Web version of this article.)

sintered at 1400 °C is 10 times decreased, compared to those samples at a lower temperature (1200 °C). Secondly, Fig. 3(b) and (c) clearly indicates that the NIR emission is enhanced (D and E components). Especially, new emission peaks are observed, which is denoted by F and G components in Fig. 3(c). The D, E, F and G emission components are located at 706 nm (~14164 cm^{-1}), 765 nm (~13060 cm^{-1}), 732 nm (~13650 cm^{-1}) and 841 nm (~11887 cm^{-1}), respectively. From the literatures, some researchers claimed that these peaks in the NIR emission region might be originated from the PL emission bands of MgO or Ta_2O_5 or defect states, e.g., oxygen vacancies [18–20].

The visible light (near blue light) emission in the wide band gap materials can be explained by the recombination process of the electrons. Defects such as oxygen vacancies in the lattice can promote the population of trapped electrons that induce the recombination process. Note that the optical band gap energy of SLMTO is reported to be 4.5–5.0 eV and SLMTO belongs to the wide band gap oxide materials. However, understanding on how specific defect states in the SLMTO host lattice improves the red and NIR emission light in the photoluminescence (PL) spectra is not clear yet.

To shed light on the increase of defects related to TaO_6 octahedral in the SLMTO powders, we measured the x-ray absorption spectroscopy (XAS) for SLMTO samples sintered at 1200 °C and 1400 °C, respectively. Fig. 4(a) shows the Ta L_3-edge (near 9.881 keV) XAS spectra for both of the SLMTO powders. The black line and red line represent the SLMTO samples sintered at 1400 °C and 1200 °C, respectively. The peaks (denoted by A and B) of the XAS spectra in the two samples do not show any significant change, specifically near the absorption edge, as shown in Fig. 4(a). Note that these two peaks are associated with the t_{2g} and e_g final states, split by the crystal field effect. The relative intensity of *A*

and *B* peaks results from the number of *d* electrons and hole. The XAS data indicates that the oxidation state of Ta is almost identical with +5 in the both of the SLMTO samples [21].

To obtain clear experimental evidence in the modulation of defect states, we adopted a new advanced x-ray technique, resonant inelastic x-ray scattering (RIXS), as shown in Fig. 4(b) and (c). In the RIXS setup, we use an energy-tuned incident photon energy, which resonates with L_3 absorption edge of specific Ta element. This photon can promote a core electron to an empty valence state. Due to the core hole, the system becomes unstable. Then, electron can decay from Ta 5d to the 2p core hole. At the end of this second order scattering process, electronic excitation between 5d orbitals are created. The difference in x-ray photon energy between incident and emission is denoted by energy loss (or energy transfer). Ta in stoichiometric SLMTO has 5+ valency and 5d orbitals are fully unoccupied ($5d^0$). When oxygen vacancies related to Ta ion exist, 5d orbitals become partially occupied. We can probe Ta 5d-related defects state inside the band gap of SLMTO by RIXS at the Ta L3-absorption edge. From a technical point of view, RIXS is a unique and powerful tool to monitor the band gap and detect element-specific defect states inside the band gap of SLMTO.

Fig. 4(b) and (c) show the high resolution Ta L_3-edge RIXS spectra as functions of the incident photon energy (E_i) for SLMTO powders sintered at 1200 °C and 1400 °C, respectively. The vertical line of intensity at zero energy loss is denoted by the elastic peak. The broad excitation peaks at around 9 eV was enhanced when E_i is tuned near the primary XAS peak. The RIXS spectra can reveal the overall structure of the unoccupied states and band gap of SLMTO samples. Fig. 5 (the inset of Fig. 5) shows the clear band gap (4.5–5 eV). No observable peak can be found below the band gap in Fig. 4(b) and (c), and Fig. 5, clearly specifying that there is little and negligible Ta-related defect in both samples for the formation of Ta 5d states. Remarkably, the amount of Ta-related defect states in the SLMTO sample sintered at 1400 °C are nearly the same with that of the sample sintered at 1200 °C. Therefore, we can claim that the Ta-related defects are uncorrelated with the enhanced NIR region in the PL spectra. For the microscopic origin of enhanced NIR region, we ruled out the possibility of Ta-related defects scenario.

4. Conclusion

In summary, we investigated structural and photoluminescence (PL) properties of $SrLaMgTaO_6$ (SLMTO) double perovskite powder samples sintered at different temperatures (1200 °C and 1400 °C) for white light emitting device (LED) application. All corresponding XRD peaks in both SLMTO samples were well indexed to a monoclinic double perovskite structure with P21/n space group. We observed a different PL spectra in the two SLMTO samples; the PL spectra of the sample sintered at higher temperature (1400 °C) exhibit suppressed blue light region and the increase of near infrared (NIR) region, compared with those samples at a lower temperature (1200 °C). To examine the scenario of Ta-related defects, we performed x-ray absorption spectroscopy and resonant inelastic x-ray scattering. RIXS results clearly show no observable Ta-related defect states in the both samples and suggest the weak relationship between the Ta-related defects and enhancement of the PL spectra.

Acknowledgments

This work was supported by a Research Grant of Pukyong National University in 2016.

References

[1] I.H. Cho, G. Anoop, D.W. Suh, S.J. Lee, J.S. Yoo, On the stability and reliability of $Sr_{1-x}Ba_xSi_2O_2N_2:Eu^{2+}$ phosphors for white LED applications, Opt. Mater. Express 2 (2012) 1292.
[2] R. Praveena, L. Shi, K.H. Jang, V. Venkatramu, C.K. Jayasankar, H.J. Seo, Sol–gel synthesis and thermal stability of luminescence of $Lu_3Al_5O_{12}:Ce^{3+}$ nano-garnet, J. Alloy. Comp. 509 (2011) 859–863.
[3] C. Shen, C. Zhong, J. Ming, YAG: Ce^{3+}, Gd^{3+} nano-phosphor for white light emitting diodes, J. Exp. Nanosci. 8 (2013) 54–60.
[4] Y. Hu, W. Zhuang, H. Ye, D. Wang, S. Zhang, X. Huang, A novel red phosphor for white light emitting diodes, J. Alloy. Comp. 390 (2005) 226–229.
[5] T. Senden, E.J. van Harten, A. Meijerink, Synthesis and narrow red luminescence of $Cs_2HfF_6:Mn^{4+}$, a new phosphor for warm white LEDs, J. Lumin. 194 (2018) 131–138.
[6] Y. Guo, B. Kee Moon, S. Heum Park, J. Hyun Jeong, J. Hwan Kim, K. Jang, R. Yu, A red-emitting perovskite-type $SrLa_{(1-x)}MgTaO_6:_xEu^{3+}$ for white LED application, J. Lumin. 167 (2015) 381–385.
[7] D.R. Kim, S.W. Park, B.K. Moon, S.H. Park, J.H. Jeong, H. Choi, J.H. Kim, The role of Yb^{3+} concentrations on Er^{3+} doped $SrLaMgTaO_6$ double perovskite phosphors, RSC Adv. 7 (2017) 1464–1470.
[8] Y. Il Kim, P.M. Woodward, Crystal structures and dielectric properties of ordered double perovskites containing Mg^{2+} and Ta^{5+}, J. Solid State Chem. 180 (2007) 2798–2807.
[9] S. Kato, E. Ohmorit, Y. Suzuki, Y. Ohshima, M. Sugai, H. Takizawa, T. Endo, Cation ordering in the oxygen deficient perovskite $Sr_{2-x}La_xMg_{1-y}Ta_{1+y}O_z$, J. Ceram. Soc. Japan 107 (1999) 209–214.
[10] S.H. Chang, Y.J. Chang, S.Y. Jang, D.W. Jeong, C.U. Jung, Y.-J. Kim, J.-S. Chung, T.W. Noh, Thickness-dependent structural phase transition of strained $SrRuO_3$ ultrathin films: the role of octahedral tilt, Phys. Rev. B 84 (2011) 104101.
[11] S.H. Chang, N. Danilovic, K.-C. Chang, R. Subbaraman, A.P. Paulikas, D.D. Fong, M.J. Highland, P.M. Baldo, V.R. Stamenkovic, J.W. Freeland, J.A. Eastman, N.M. Markovic, Functional links between stability and reactivity of strontium ruthenate single crystals during oxygen evolution, Nat. Commun. 5 (2014) 4191.
[12] L.J.P. Ament, M. van Veenendaal, T.P. Devereaux, J.P. Hill, J. van den Brink, Resonant inelastic x-ray scattering studies of elementary excitations, Rev. Mod. Phys. 83 (2011) 705–767.
[13] M.Y. Jeong, S.H. Chang, B.H. Kim, J.-H. Sim, A. Said, D. Casa, T. Gog, E. Janod, L. Cario, S. Yunoki, M.J. Han, J. Kim, Direct experimental observation of the molecular J eff= 3/2 ground state in the lacunar spinel $GaTa_4Se_8$, Nat. Commun. 8 (2017) 782.
[14] B.H. Toby, R factors in Rietveld analysis: how good is good enough? Powder Diffr. 21 (2006) 67–70.
[15] J.Y. Park, J.S. Joo, H.K. Yang, M. Kwak, Deep red-emitting $Ca_{14}Al_{10}Zn_6O_{35}:Mn^{4+}$phosphors for WLED applications, J. Alloy. Comp. 714 (2017) 390–396.
[16] W. Ran, H.M. Noh, B.K. Moon, S.H. Park, J.H. Jeong, J.H. Kim, G. Liu, J. Shi, Crystal structure, electronic structure and photoluminescence properties of $KLaMgWO_6:Eu^{3+}$phosphors, J. Lumin. 197 (2018) 270–276.
[17] T. Horikubi, H. Watanabe, N. Kamegashira, Structure of perovskite type compounds, $ALaMnTaO_6$ (A=Sr, Ba), J. Alloy. Comp. 274 (1998) 122–127.
[18] N. Jain, N. Marwaha, R. Verma, B.K. Gupta, A.K. Srivastava, Facile synthesis of defect-induced highly-luminescent pristine MgO nanostructures for promising solid-state lighting applications, RSC Adv. 6 (2016) 4960–4968.
[19] N. Pathak, P.S. Ghosh, S.K. Gupta, R.M. Kadam, A. Arya, Defects induced changes in the electronic structures of MgO and their correlation with the optical properties: a special case of electron–hole recombination from the conduction band, RSC Adv. 6 (2016) 96398–96415.
[20] H. Shin, S.Y. Park, S.T. Bae, S. Lee, K.S. Hong, H.S. Jung, Defect energy levels in Ta_2O_5 and nitrogen-doped Ta_2O_5, J. Appl. Phys. 104 (2008) 5–7.
[21] T.K. Mandal, V.V. Poltavets, M. Croft, M. Greenblatt, Synthesis, structure and magnetic properties of $A_2MnB'O_6$(A=Ca, Sr; B′=Sb, Ta) double perovskites, J. Solid State Chem. 181 (2008) 2325–2331.